Sediment failure of St. Pierre Slope: new insights of failure mechanisms and slope instability due to the 1929 Grand Banks Earthquake

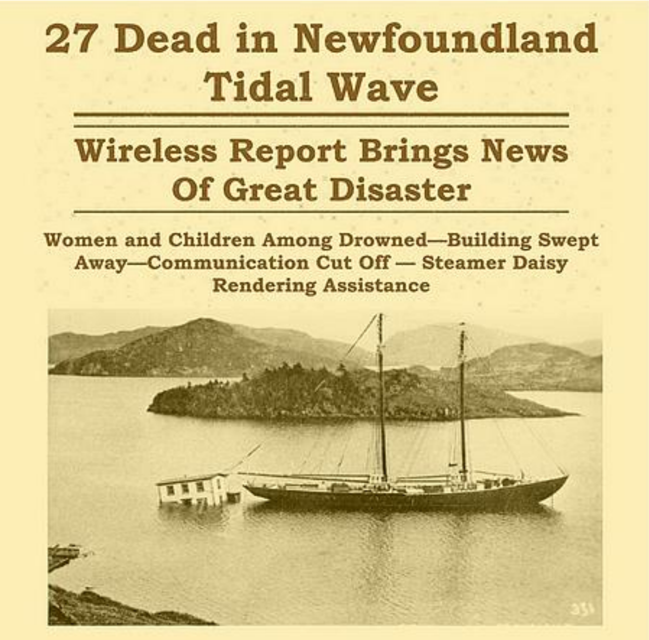
27 Dead in Newfoundland Tidal Wave

Wireless Report Brings News Of Great Disaster

Women and Children Among Drowned—Building Swept Away—Communication Cut Off — Steamer Daisy Rendering Assistance

Schulten, I.[1], Mosher D. C.[2], Piper, D. J. W.[2], Krastel, S[3]. and MacKillop, K.[2]


The Free Press.

Known Dead Total Twenty-Seven and Property Loss is Enormous

Tidal Wave Sweeps East Coast Burin

Magistrate Hollett Reports To Govt.

Telegraph Office is Anchored in Harbor

EGU2020 – 15909
session: NH5.6

1) Department of Oceanography, Dalhousie University, Halifax, Canada
2) Natural Resources Canada, Bedford Institute of Oceanography, Dartmouth, Canada
3) Institute of Geosciences, Christian-Albrechts-Universität zu Kiel, Kiel, Germany

May 4th, 2020

The 1929 event & the St. Pierre Slope

On November 18th 1929 a M_w 7.2 strike-slip earthquake (★; <20 cm of vertical displacement) occurred in ~20 km depth underneath the Laurentian Fan of the southwestern Grand Banks of Newfoundland (Bent, 1995). This earthquake caused a submarine landslide, which led to the first observation of naturally occurring turbidity currents and is one of the few landslides known to have caused a tsunami. The turbidity current broke 12 transatlantic tele-communication cables and the tsunami killed 28 people and destroyed onshore infrastructure, especially on Burin Peninsula of Newfoundland.

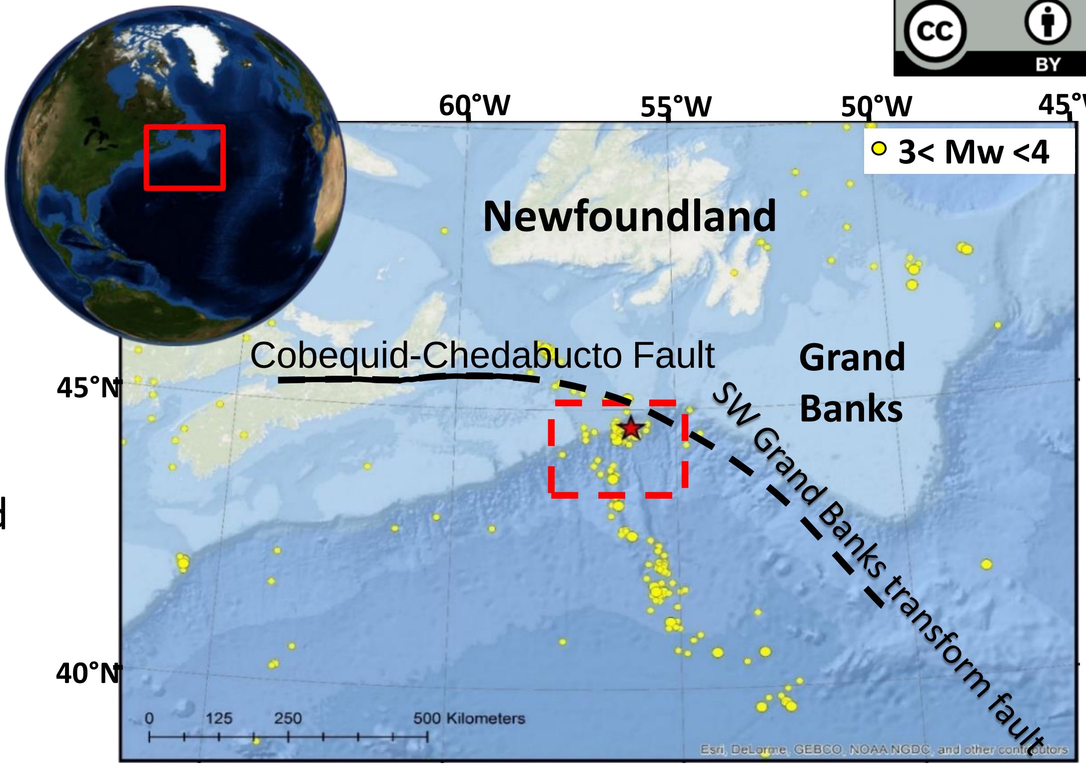

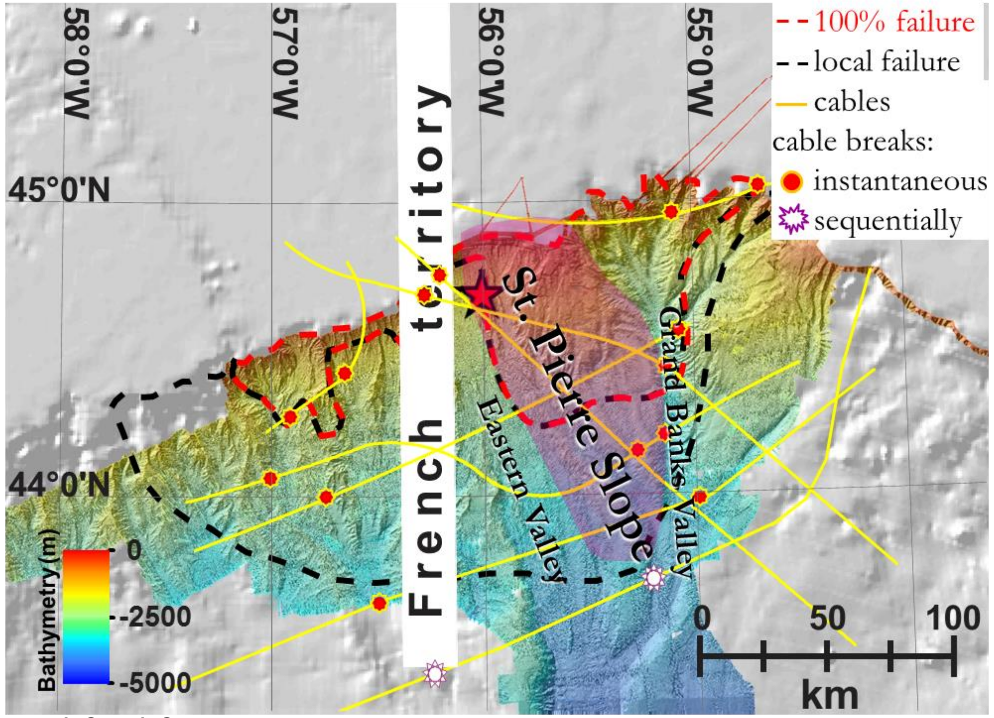

Modified from Piper, 2009

The 1929 submarine landslide is described as follow:

- **widespread, translational + retrogressive sediment failure = <25 m-thick** (Piper et al., 1999; Mosher & Piper, 2007; Schulten et al., 2018)
- **rapid flow transformation** into turbidity currents (Piper et al., 1999)
- **volume estimate: ~100 km³**,~40% entered the turbidity currents (Piper & Aksu, 1987; McCall, 2006; Schulten et al., 2018)
- **main failure area = St. Pierre Slope (Piper et al., 1999)**
  - numerous shallow escarpments in >730 m water depth (mwd)
  - numerous incised valleys & canyon systems

Objective & Methods

Open question: water depth of surficial failure, their thin nature and rapid flow transition contradict what might be expected for a tsunamigenic event

Objective: Need to understand characteristics of initial sediment failure = failure dimensions, kinematics, slope stability

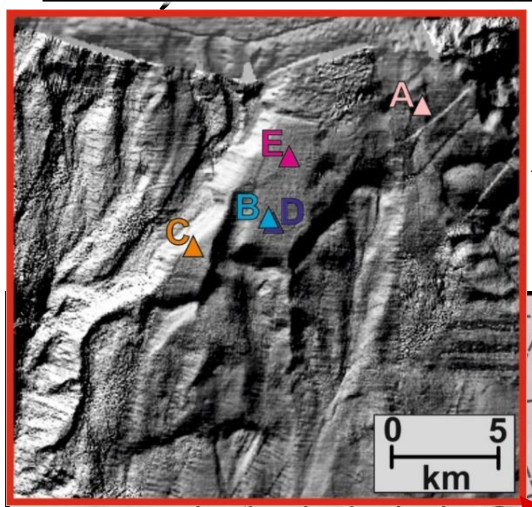

Core locations (A-E), upper St. Pierre Slope

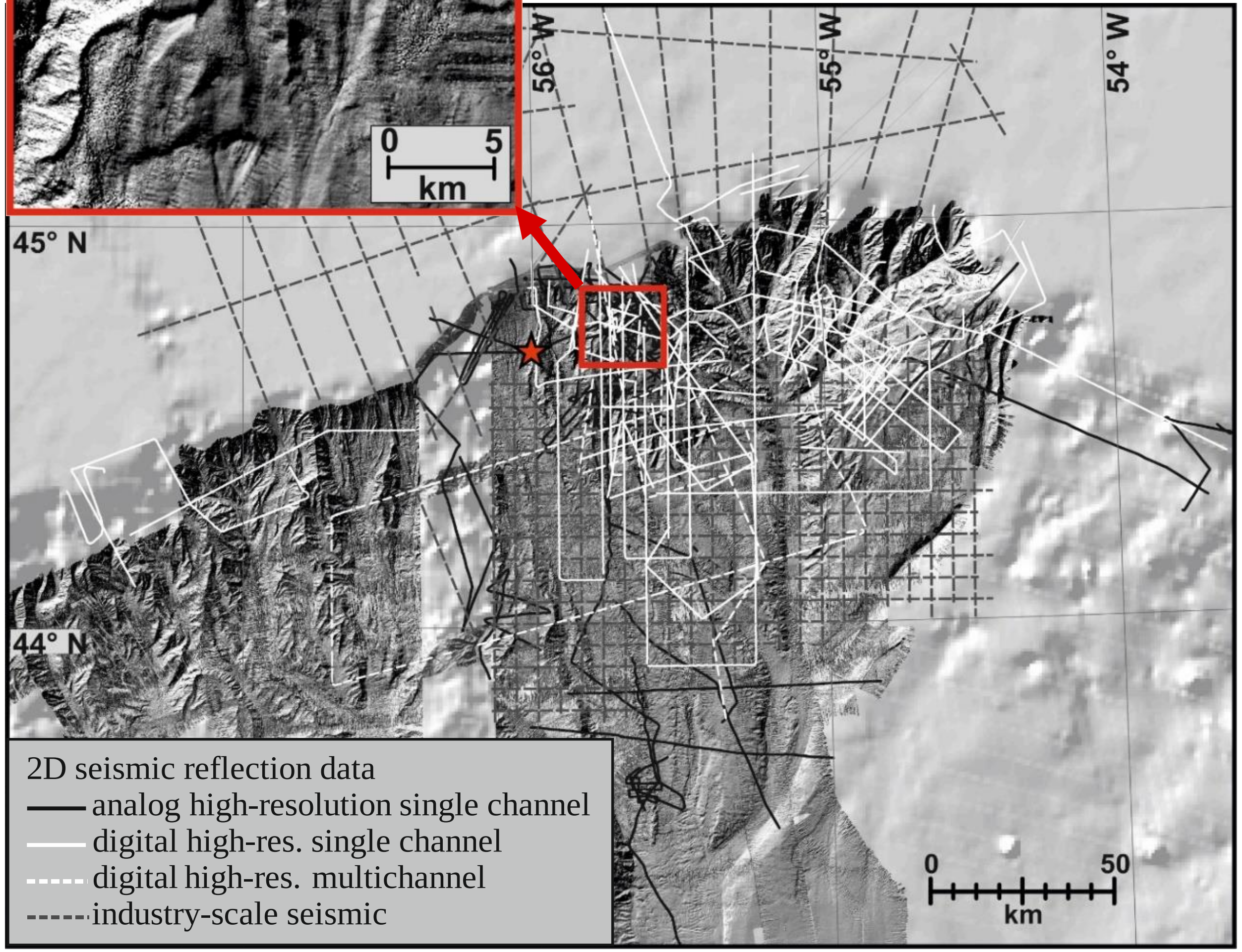

Modified from Schulten et al., 2019

Data source = legacy + newly acquired data (1985-2015):

- multibeam swath bathymetry
- ultra high-resolution seismic data
- 2D seismic reflection data (high-resolution & industry-scale)
- 5 x marine gravity cores from the unfailed part of the slope (~500-730 mwd)

I. Seismic reflection data and multibeam data analysis; published in Schulten et al. (2019)

- establishing a full stratigraphy St. Pierre Slope using results of previous publications
- identification of previously unrecognized sub-bottom structures

Objective & Methods

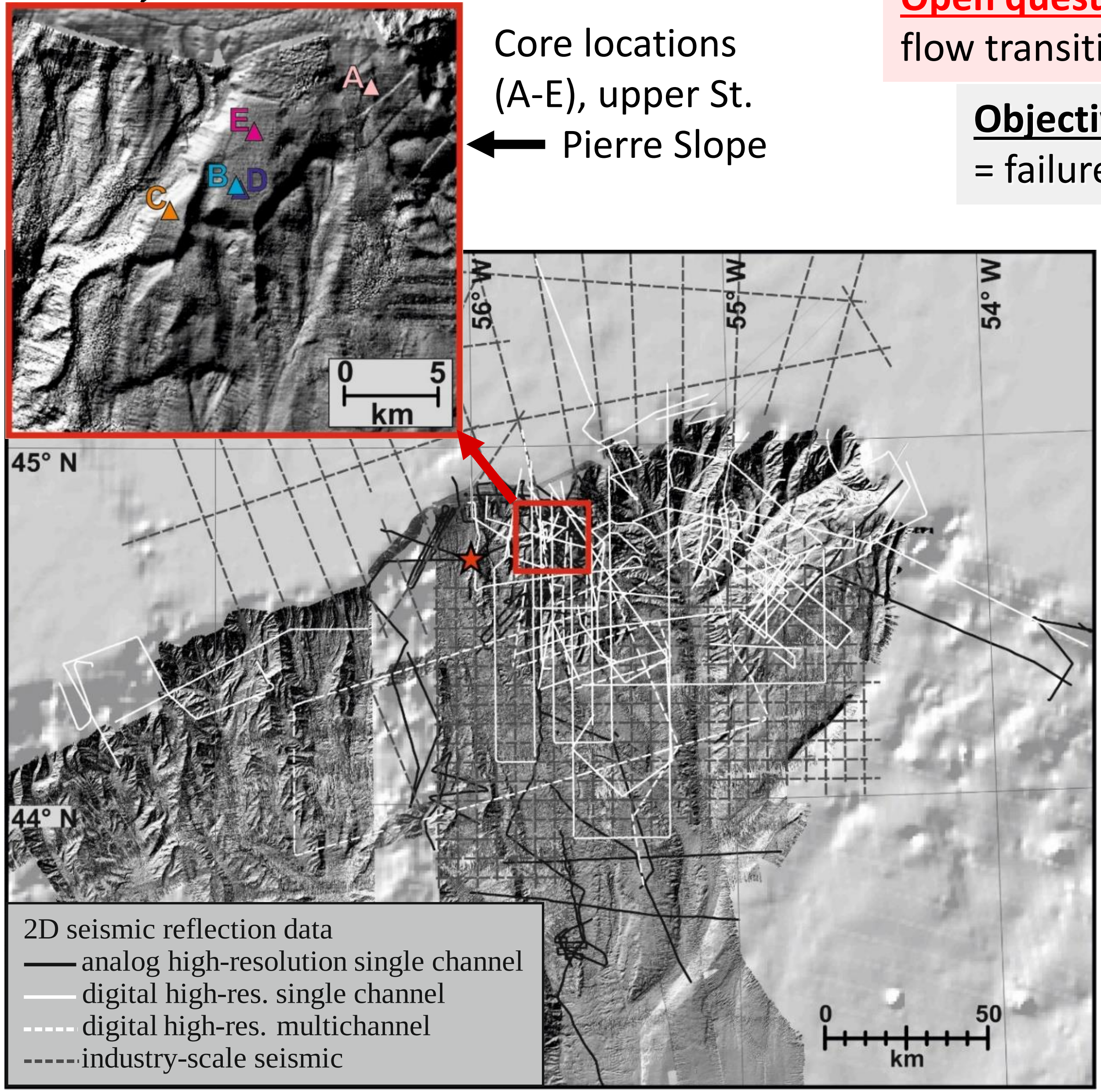

Core locations (A-E), upper St. Pierre Slope

Modified from Schulten et al., 2019

Open question: water depth of surficial failure, their thin nature and rapid flow transition contradict what might be expected for a tsunamigenic event

Objective: Need to understand characteristics of initial sediment failure = failure dimensions, kinematics, slope stability

Data source = legacy + newly acquired data (1985-2015):

- multibeam swath bathymetry
- ultra high-resolution seismic data
- 2D seismic reflection data (high-resolution & industry-scale)
- 5 x marine gravity cores from the unfailed part of the slope (~500-730 mwd)

II. Geotechnical (consolidation, triaxial, shear strength testing) & static and pseudo-static infinite slope stability analysis

= sediment cores + sediment slabs (2-550 m-thick)

- FOS for sediment slabs = from normalized shear strength (Su_{NSP}; triaxial results) + effective stress ($P'_{vo\ trend}$) calculated using an equation of Kominz et al. (2011)
- PGA to magnitude-distance conversion = equations from Atkinson and Boore (2006, AB2006) and Campbell and Bozorgnia (2008; CB2008)

Results + Interpretation

I. Seismic reflection data & multibeam swath bathymetry (Schulten et al., 2019)

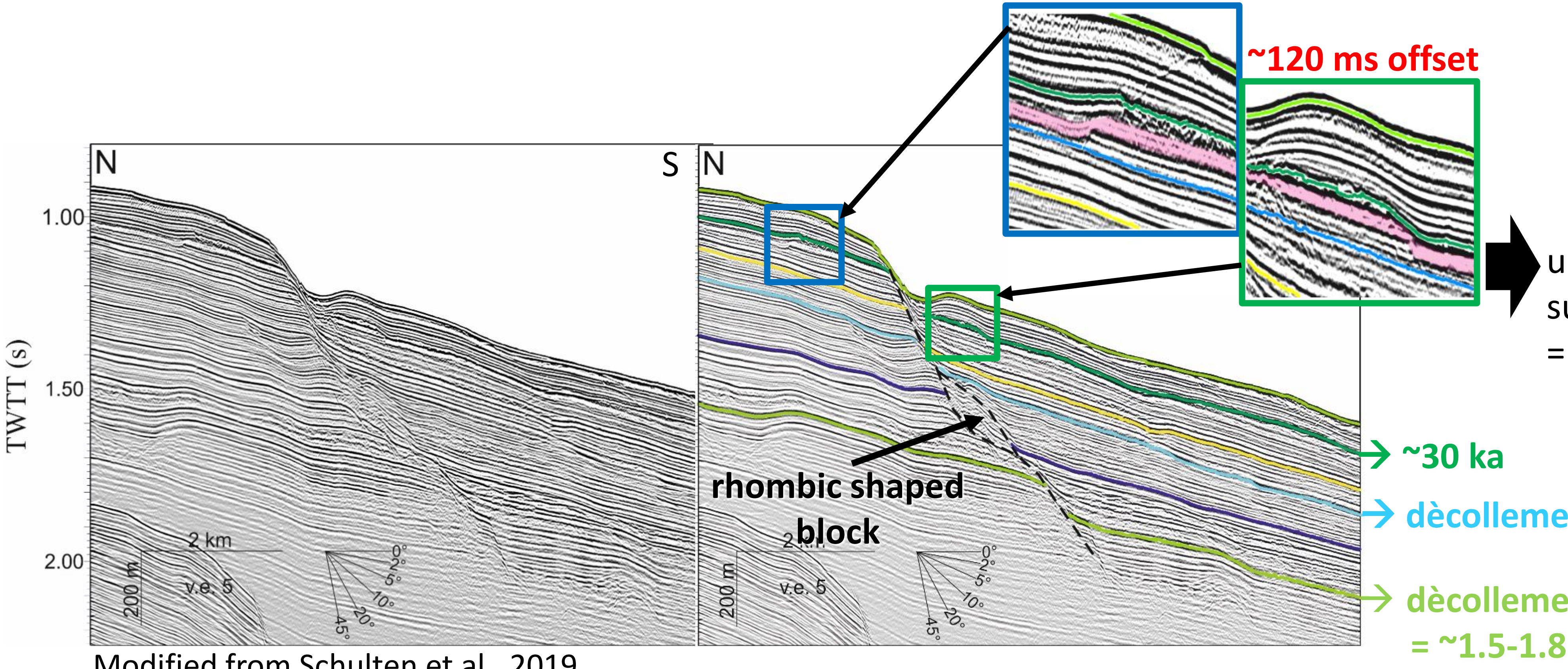

Modified from Schulten et al., 2019

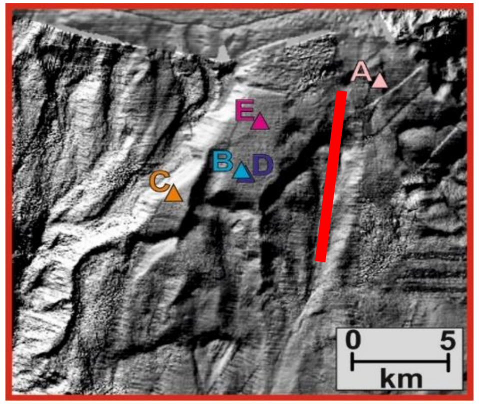

upper strata down to ~100 m sub-bottom depth (mbsf)
= consistent stratigraphy and interval thicknesses to both sites of the reflection offset

at St. Pierre Slope reflection offsets (black dashed line) are evident underneath modern seafloor escarpments down to a depth of ~700 ms or 400-550 m (near the green reflector) (Schulten et al., 2019)

low angle (~17°), normal faults (Schulten et al., 2019):

- ~100 m vertical displacement (Schulten et al., 2019)
- rupture the modern seafloor (Schulten et al., 2018)
- down to different depths within the Quaternary section of the slope (Schulten et al., 2019)

Results + Interpretation

I. Seismic reflection data & multibeam swath bathymetry (Schulten et al., 2019)

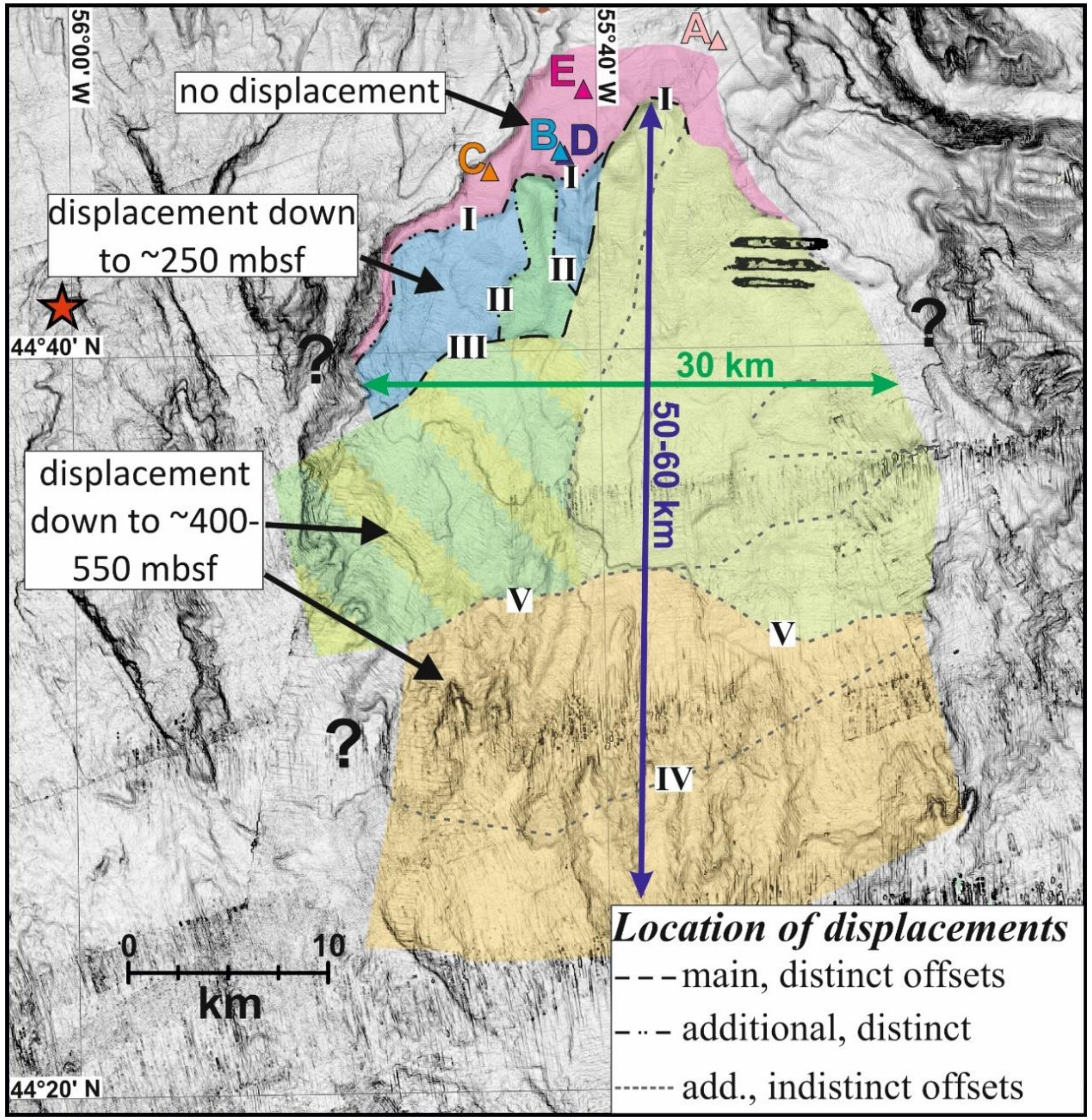

Modified from Schulten et al., 2019

faults are part of a massive (~560 km³), complex slump with multiple décollements (250 mbsf & 400-550 mbsf) and slumping towards S & SW (Schulten et al., 2019)

~250 mbsf dècollement (light blue horizon) = ~470 ka (MIS 12; Piper et al., 2005)

- regional unconformity = denotes a change in depositional characteristic as a result of shelf-crossing glaciers + increased sedimentation rate
- overlies thick (30-40 m) mass transport deposits (MTD`s) (Schulten et al., 2019)

400-550 mbsf dècollement (light green to yellow horizon) = ~1.5-1.8 Ma (early Pleistocene; Piper & Normark, 1982)

- overlain by ~40 m-thick MTDs in the shallower part of the slope (Schulten et al., 2019)
- underlain by sediment waves further downslope (Piper et al., 2005; Schulten et al., 2019)

Results + Interpretation

II. Geotechnical analysis & infinite slope stability analysis

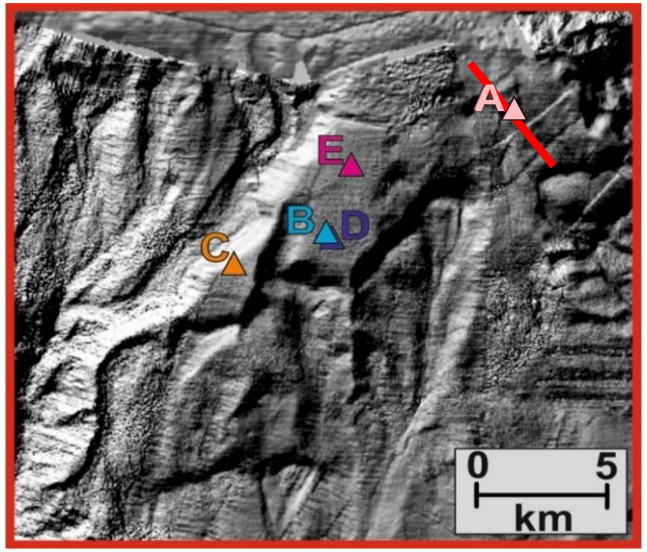

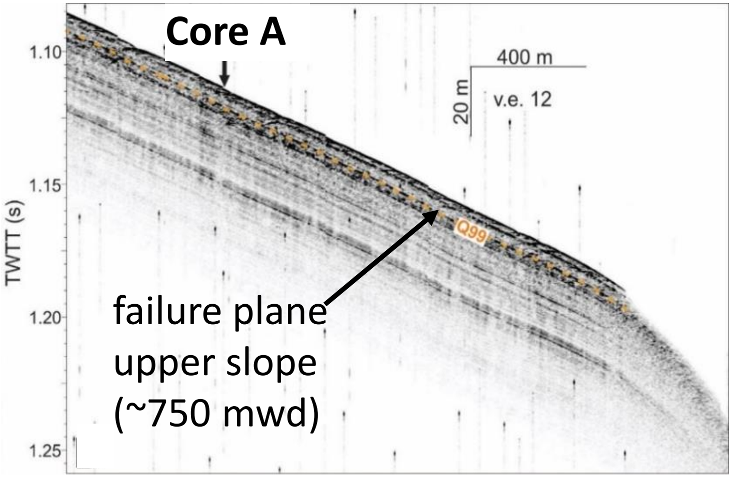

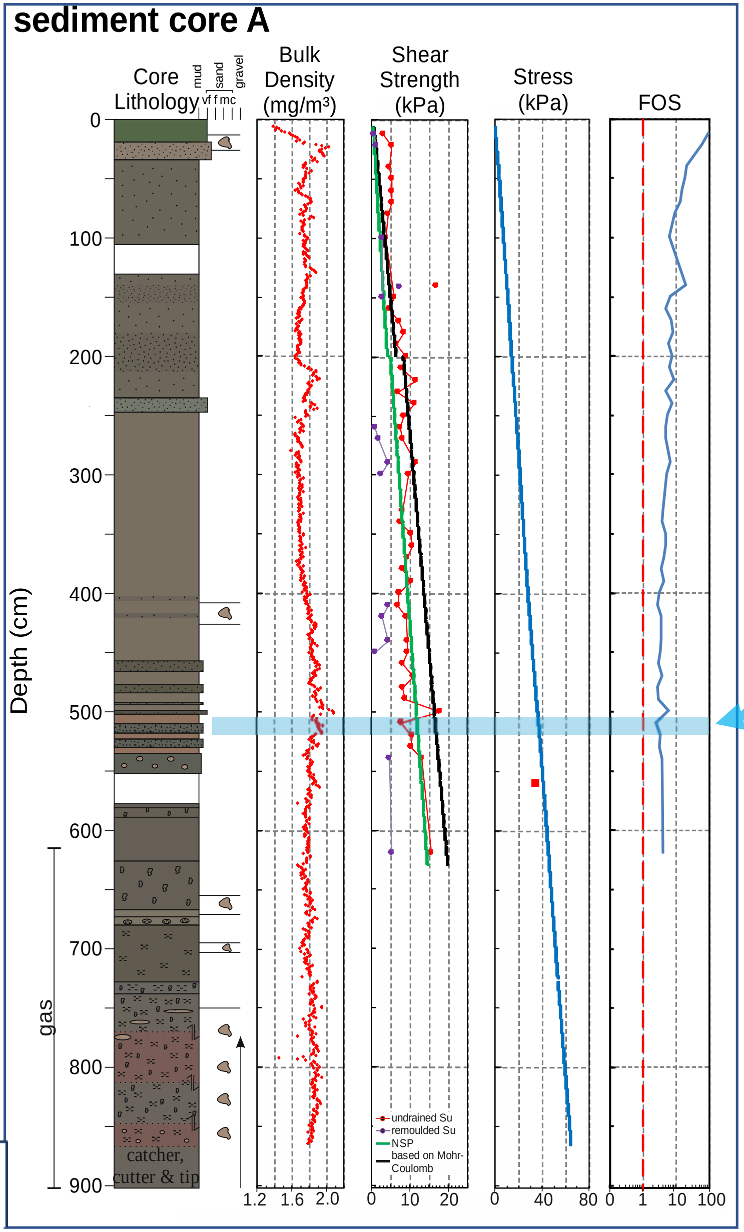

1. mainly bioturbated, muddy (silt + clay) sediment
   → interbedded sandier or siltier layers are abundant in 400 to 600 cm core depth = MTD`s or sandy turbidites
   → gas expansion cracks are evident in >600 cm, capped by the overlying MTD`s
2. FOS minima = lithological changes between MTD`s or sandy turbidites and clay-rich mud that show different shear strengths
3. failure plane at the upper St. Pierre Slope in ~10 m depth = core section with gas expansion cracks
4. OCR = 0.76-0.89 from 3 to 9 m = normal (NC) to slight underconsolidation (UC)

UC as result of excess pore pressure + formation of weak layers due to:

1) **high sedimentation rates**
2) **rapidly deposited MTD`s or sandy turbidites**
3) **presence of gas**

Results + Interpretation

II. Geotechnical analysis & infinite slope stability analysis

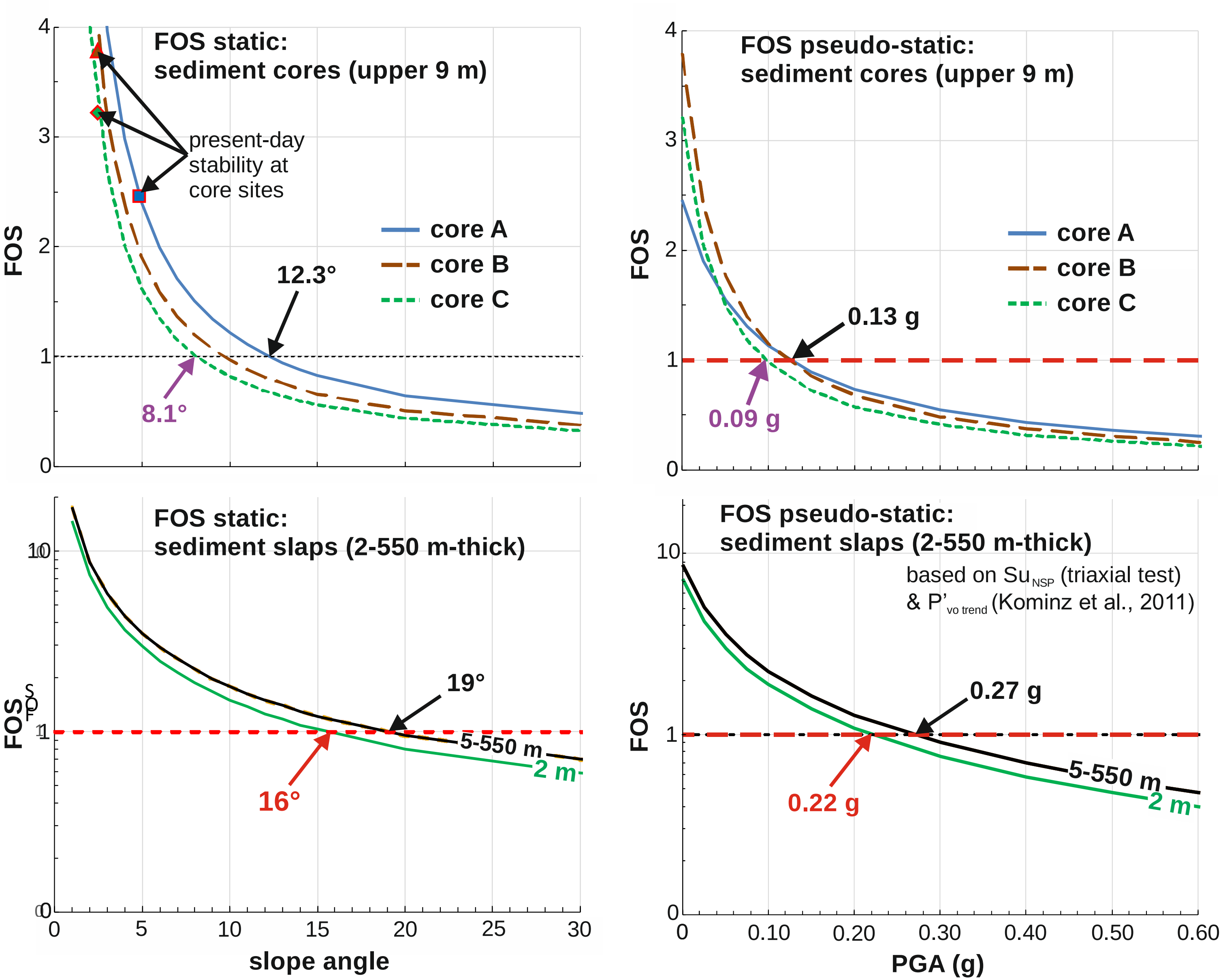

FOS of sediment cores
= 8.1°
= 0.09 g

→present-day slope angle at St. Pierre Slope
= 2-5°, steeper only on canyon walls

slope is stable under static and present-day conditions

FOS of sediment slabs (2-550 m-thick)
= 16°
= 0.22 g for a 2 m
& 0.27 g for 5-550 m-thick slabs

Results + Interpretation

II. Geotechnical analysis & infinite slope stability analysis

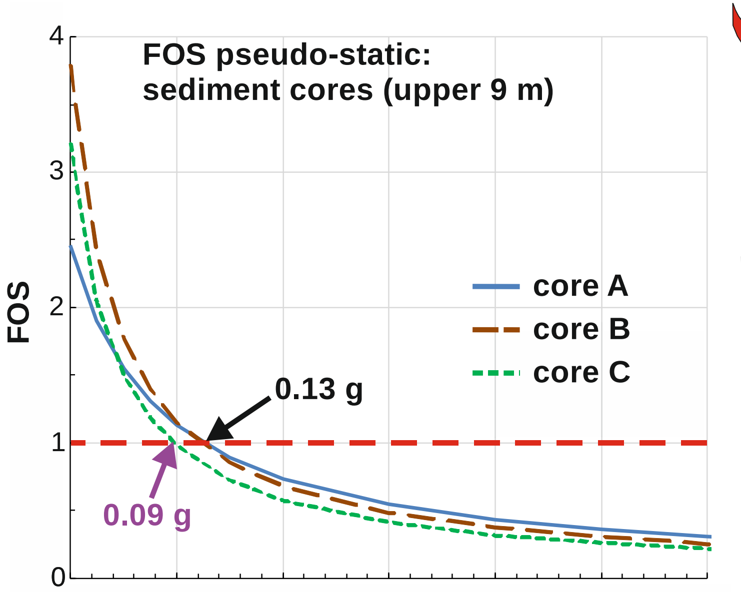

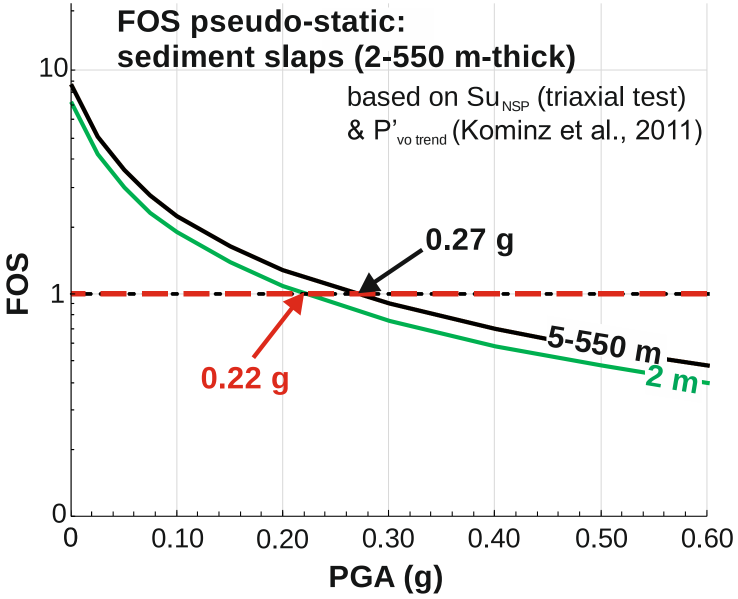

PGA of 0.09 g = M_w>4.8, <5 km distance

= minimum earthquake loading required to cause slope instability under present-day conditions

= earthquakes past 30 yrs = M_w<4, >5 km distance

1929 earthquake = M_w 7.2, ~26 km distance

= 0.2 g AB2006 or 0.13 g CB2008:

sed. cores = failure

core data include shear strength reductions, additional factors are present (e.g. weak layers)

slabs >10 m = stable

Su_{NSP} + $P`_{vo\ trend}$ (corr. for diagenesis) → slope stability in response to earthquake loading, no additional factors (e.g. weak layers, cyclic loading)

1929 earthquake: ≠ slump

≠ surficial failures >10 m

additional factors are needed to explain failure in 1929 = presence of weak layers

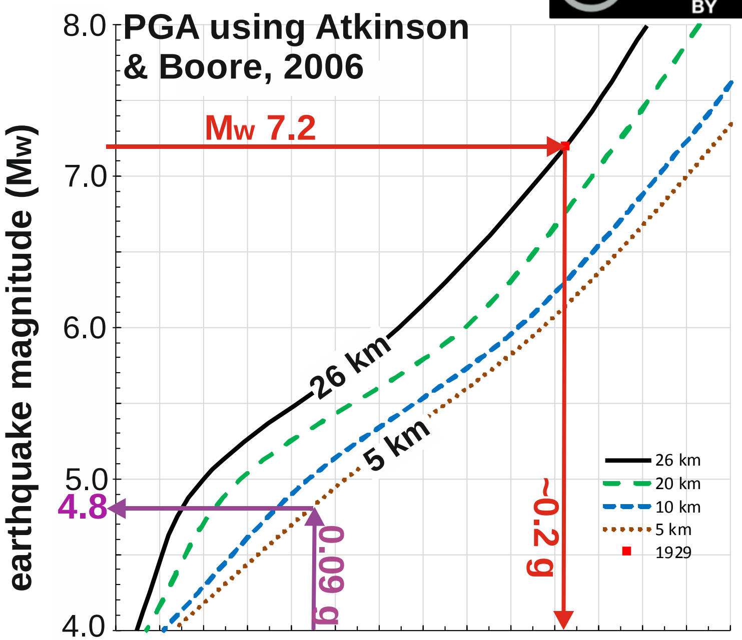

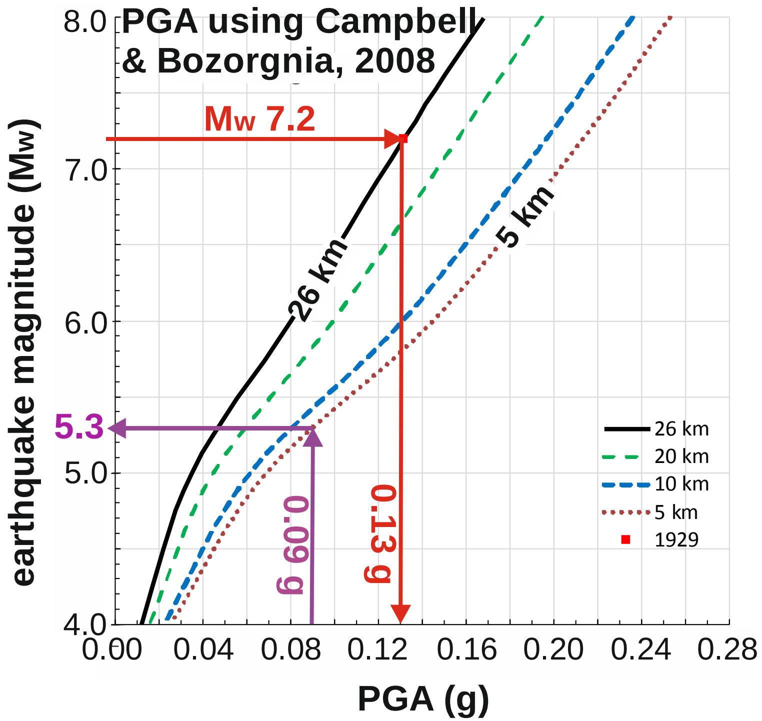

Conclusions

- at St. Pierre Slope planar-normal faults occur down to ~550 mbsf and are part of a complex, massive (~560 km³) slump
  = recent activity, as faults rupture the modern seafloor & height of seafloor escarpments matches the total vertical displacement along the faults (Schulten et al., 2019)

- combination of earthquake loading & pre-conditioning factors is necessary to cause slope instability at St. Pierre Slope

- geomechanical weak layers are a consequence of UC in connection with excess pore pressure

  décollements of the slump (250 mbsf & 400-550 mbsf) are associated with MTD's and sediment waves that likely form weak layers susceptible to excess pore pressure development in response to earthquake loading

- 1929 earthquake = displacement of the slump (550 m-thick block) + surficial (<25 m-thick) failures

  = potential liquifaction within sediment waves + UC in connection with mass deposition and development of excess pore pressure in response to earthquake loading is necessary to explain failure

  likely a more effective source for tsunami generation than the translational, shallow (<25 m) failures
  = tsunami simulation by Løvholt et al. (2018) supports hypothesis that slumping + surficial failures occurred in 1929

Please feel free to comment in the chat or contact me via email at Irena.Schulten@dal.ca

Acknowledgements

I. Schulten was supported by NSERC CREATE Transatlantic Ocean System Science and Technology (TOSST) grant and NSERC Discovery Grants to D. C. Mosher and D.J. W. Piper. Different data sets were provided by the Geological Survey of Canada Atlantic (GSCA, Natural Resources) and DFG funded Expedition MSM45 (Schneider) & MSM47 (S. Krastel). Thanks to the researchers at BIO and Marum for their help with analysing and describing the cores. Thanks goes especially to K. MacKillop, A. Kopf and G. Wiemer.

DALHOUSIE UNIVERSITY *Inspiring Minds*

TOSST TRANSATLANTIC RESEARCH SCHOOL

CANADA 1842 GEOLOGICAL SURVEY - COMMISSION GÉOLOGIQUE

Natural Resources Canada Ressources naturelles Canada

Canada

NSERC CRSNG

References

Atkinson, G. M., and Boore, D. M., 2006. Earthquake Ground-Motion Prediction Equations for Eastern North America. Bulletin of the Seismological Society of America, Vol. 96, p. 2181-2205.

Bent, A. L., 1995. A complex double-couple source mechanism for the Ms 7.2 1929 Grand Banks earthquake. Bulletin of the Seismological Society of America, Vol. 85, p. 1003-1020. Geological Survey of Canada Atlantic, 2011. The 1929 “Grand Banks” Earthquake and Tsunami, Geological Surevez of Canada, Natural Resources Canada Geofacts [new series].

Campbell, K. W., and Bozorgnia, Y., 2008. NGA ground motion model for the geometric mean horizontal component of PGA, PGV, PGD and 5% damped linear elastic response spectra for periods ranging from 0.01to 10 s. Earthquake Spectra, Vol. 24, p. 139–171.

Kominz, M. A., Patterson, K., and Odette, D., 2011. Lithology dependence of porosity in slope and deep marine sediments. Journal of Sedimentary Research, Vol. 81, p. 730-742. Doi: 10.2110/jsr.2011.60.

Løvholt, F., Schulten, I., Mosher, D., Harbitz, C., and Krastel, S., 2018. Modelling of the 1929 Grand Banks slump and landslide tsunami. From: Lintern, D. G., Mosher, D. C., et al. (eds). Subaqueous Mass Movements. Geological Society, London, Special Publications, 477, https://doi.org/10.1144/SP477.28.

McCall, C. W., 2006. A Geological and Geophysical study of the 1929 Grand Banks slide. Master Thesis, Saint Mary’s University, Halifax, Nova Scotia.

Mosher, D. C., and Piper, D. J. W., 2007. Analysis of Multibeam seafloor imagery of the Laurentian Fan and the 1929 Grand Banks landslide area. In: Lykousis, V., Sakellariou, D., and Locat, J. (eds.), Submarine Mass Movements and Their Consequences, 3rd International Symposium. Advances in Natural and Technological Hazards Research, Springer, Vol. 27, p.77-88.

Piper, D. J. W., and Normark, W. R., 1982. Acoustic interpretation of Quaternary sedimentation and erosion on the channelled upper Laurentian Fan, Atlantic margin of Canada. Canadian Journal of Earth Sciences, Vol. 19, p. 1974-1984.

Piper, D. J. W., and Aksu, A. E., 1987. The source and origin of the 1929 Grand Banks turbidity current inferred from sediment budgets. Geo-Marine Letters, Vol. 7, p. 177-182.

Piper, D. J. W., Cochonat, P., and Morrison, M. L., 1999. The sequence of events around the epicentre of the 1929 Grand Banks earthquake: initiation of debris flows and turbidity current inferred from sidescan sonar. Sedimentology, Vol. 46, p. 79-97.

Piper, D. J. W., Macdonald, A. W. A., Ingram, S., Williams, G. L., and McCall, C., 2005. Late Cenozoic architecture of the St. Pierre Slope. Canadian Journal of Earth Sciences, Vol. 42, p. 1987-2000, doi:10.1139/E05-059.

Schulten, I., Mosher, D. C., Krastel, S., Piper, D. J. W., and Kienast, M., 2018. Surficial sediment failures due to the 1929 Grand Banks Earthquake, St Pierre Slope. In: Lintern, D. G., Mosher, D. C., et al. (eds), 2019 Subaqueous Mass Movements and Their Consequences: Assessing Geohazards, Environmental Implications and Economic Significance of Subaqueous Landslides. Geological Society, London, Special Publications, 477, p. 583-596, https://doi.org/10.1144/SP477.25.

Schulten, I., Mosher, D. C., Piper, D. J. W., and Krastel, S., 2019. A massive slump on the St. Pierre Slope, a new perspective on the 1929 Grand Banks submarine landslide. Journal Geophysical Research: Solid Earth, Vol. 124, p. 7538-7561, doi: 10.1029/2018JB017066.